FIFTH INTERNATIONAL CONGRESS ON SOUND AND VIBRATION
DECEMBER 15-18, 1997
ADELAIDE, SOUTH AUSTRALIA

USE OF DIRECTIONAL SPECTRA OF VIBRATION SIGNALS FOR DIAGNOSIS OF MISALIGNMENT IN ROTATING MACHINERY

Chong-Won Lee, Yun-Sik Han, and Young-Seob Lee

Center for Noise and Vibration Control(NOVIC), Department of Mechanical Engineering
KAIST, Science Town, Taejon, 305-701, KOREA
Tel : 82-42-869-3016, Fax : 82-42-869-8220, E_mail : cwlee@hanbit.kaist.ac.kr

In this paper, a new vibration signal processing technique is applied to a laboratory rotor system for characterization of its misalignment. This technique utilizes the directional spectra of the complex-valued vibration signals measured from two vibration transducers, placed perpendicular to each other. The directional power spectrum preserves the important directivity and shape information of whirling orbits, whereas the phase of the directional cross-spectrum indicates its inclination angle. Experimental results support that the directional power- and cross-spectra can be effectively used for diagnosis of the misalignment in test rig.

INTRODUCTION

The operational vibration monitoring in rotating machinery gives useful information about machinery malfunctions. Although the orbits taken from a rotor well represent the planar motions, they are usually complicated in shape, containing many frequency components, so that it is not straight forward to relate them with any potential malfunctions. Spectral analysis is probably the most popular signal processing technique for diagnosing the rotor systems because the frequency components and the corresponding amplitudes vary in accordance with various fault mechanisms. Conventional spectral analysis techniques enable the display of the corresponding frequency contents in a systematic way, but they treat the rotor vibrations as real quantities so that their frequency spectra lose such an important orbital information as directivity, i.e. *forward* (the same direction as the rotor rotation) or *backward* (the direction opposite to the rotor rotation). On the other hand, the *directional power spectra* (dPS) of complex-valued signals, which preserve the important directivity and shape information of planar motion, has proven to be a powerful diagnostic tool for rotating and reciprocating machinery [1-8]. The key idea is that, in general, a planar whirling can be decomposed into *forward* and *backward* harmonic components and that the harmonic components, *backward* or *forward*, can be directly identified in the dPS which is acquired from the Fourier transform of the complex-valued signal representing the planar motion of the rotor. The complex-valued signal is usually made up with two real-valued signals measured from two vibration transducers, placed perpendicular to each other. The positive (negative) frequency components appearing in dPS physically correspond to forward (backward) whirling components. Thus the variations in forward and backward frequency components of dPS can be effectively used for diagnosing any defects or faults in a rotating machine, which cause the change in whirl orbits or Lissajous figures. In addition to the directivity and shape information, it is necessary to determine the inclination angle of planar motion. To this end, the *directional cross-spectra* (dCS) are proposed to give the inclination angle of planar motion.

In this paper, in order to investigate the effectiveness of the proposed diagnostic method, the directional spectral analysis technique is applied to a laboratory rotor system for diagnosis of its misalignment. Misalignment , which is known to be the second most common malfunction after unbalance[9], is achieved by adjusting the bearing housing supports using the two translation stages, resulting in additional preloads. Experimental results support that the dPS and dCS can be effectively used for diagnosis of the misalignment in test rig.

COMPLEX NOTATION

In this section, we will establish the convention for representing complex signals and consider the complex harmonic components as phasors rotating in a complex plane [1-14]. Let us first consider a pair of complex conjugate signals, $p(t)$ and $\overline{p}(t)$, of the form

$$p(t) = y(t) + \mathrm{j}z(t)\,,\ \ \overline{p}(t) = y(t) - \mathrm{j}z(t)\,, \tag{1}$$

where $y(t)$ and $z(t)$ are the real signals, j $(=\sqrt{-1})$ means the imaginary number and the bar denotes the complex conjugate. It is then natural to associate the complex signal $p(t)$ with a moving point, or a moving vector drawn from the origin, in the plane whose Cartesian coordinates are $y(t)$ and $z(t)$. When we try to display the complex signal $p(t)$ geometrically in the complex plane, the y-axis becomes the real axis, the z-axis being the imaginary axis, as indicated in Figure 1. The complex harmonic signal $p(t)$ of frequency ω can be rewritten in polar form, using Euler's formula, as

$$\begin{aligned} p(t) &= y(t)+\mathrm{j}z(t) = p^f(t)+p^b(t) = r^f e^{\mathrm{j}\omega t} + r^b e^{-\mathrm{j}\omega t} \\ &= \left\{\frac{1}{2}(y_c+z_s)+\frac{\mathrm{j}}{2}(z_c-y_s)\right\}e^{\mathrm{j}\omega t} + \left\{\frac{1}{2}(y_c-z_s)+\frac{\mathrm{j}}{2}(z_c+y_s)\right\}e^{-\mathrm{j}\omega t}, \end{aligned} \tag{2}$$

where, $p^f(t) = r^f e^{\mathrm{j}\omega t}$, $p^b(t) = r^b e^{-\mathrm{j}\omega t}$, $y(t) = y_c\cos\omega t + y_s\sin\omega t$, $z(t) = z_c\cos\omega t + z_s\sin\omega t$, $r^f = |r^f| e^{\mathrm{j}\phi^f}$, $r^b = |r^b| e^{\mathrm{j}\phi^b}$. Here the superscripts b and f denote the backward(clockwise) and forward(counter-clockwise in Figure 1) components, and, y_c and y_s (z_c and z_s) are the Fourier coefficients associated with $y(t)$ ($z(t)$). Note that the complex term $e^{j\omega t}$ ($e^{-j\omega t}$) is associated with the forward (backward) rotating unity vector at the circular rotating speed of ω and that the complex quantity r^f (r^b) is associated with the vector having the amplitude, $|r^f|$ ($|r^b|$), and the initial phase, ϕ^f (ϕ^b). It is well known that the complex harmonic signal, which is the resultant of two contra-rotating vectors, each with different amplitudes and initial phases, forms an ellipse in the complex plane [14]. The shape and directivity of the elliptic planar motion are determined as follows :

$$\begin{aligned}
&r^f\ (r^b) = 0 &&: \text{ backward (forward) circular planar motion,}\\
&|r^b| > |r^f| &&: \text{ backward elliptic planar motion.}\\
&|r^b| = |r^f| &&: \text{ straight line motion,}\\
&|r^b| < |r^f| &&: \text{ forward elliptic planar motion.}
\end{aligned} \tag{3}$$

To quantify the above shape and directivity information, we may introduce the shape and directivity index (SDI) defined as

$$-1 \le \text{SDI} = \frac{|r^f| - |r^b|}{|r^f| + |r^b|} \le 1 \tag{4}$$

where the inequality relations can be easily proven. Note that

$$\begin{aligned}
\text{SDI} &= -1 &&: \text{ backward circular planar motion,}\\
-1 < \text{SDI} &< 0 &&: \text{ backward elliptic planar motion,}\\
\text{SDI} &= 0 &&: \text{ straight line motion,}\\
0 < \text{SDI} &< 1 &&: \text{ forward elliptic planar motion,}\\
\text{SDI} &= 1 &&: \text{ forward circular planar motion.}
\end{aligned}$$

In other words, the sign of SDI determines the directivity and the absolute value of SDI indicates the correlation coefficient to a circle.

The inclination angle ϕ_{inc} of the ellipse made by the major axis of the ellipse with respect to the y axis is obtained as

$$\begin{aligned}
\phi_{inc} &= \frac{1}{2}(\phi^f + \phi^b). \\
&= \frac{1}{2}\left[\text{Tan}^{-1}\frac{z_c - y_s}{y_c + z_s} + \text{Tan}^{-1}\frac{z_c + y_s}{y_c - z_s}\right] = \frac{1}{2}\text{Tan}^{-1}\frac{2(y_c z_c + y_s z_s)}{y_c^{\,2} + y_s^{\,2} - z_c^{\,2} - z_s^{\,2}}.
\end{aligned} \tag{5}$$

The major and minor radii of the ellipse are

$$|r|_{maj} = |r^f| + |r^b|, \quad |r|_{min} = \big||r^f| - |r^b|\big| \tag{6}$$

where, $\left|r^f\right| = \frac{1}{2}\sqrt{\left(z_s + y_c\right)^2 + \left(z_c - y_s\right)^2}$ and $\left|r^b\right| = \frac{1}{2}\sqrt{\left(y_s + z_c\right)^2 + \left(y_c - z_s\right)^2}$. Therefore, in order to identify the parameters of the elliptic planar motion, we need to acquire the shape, directivity and inclination angle associated with the planar motion.

DIRECTIONAL SPECTRA

The directional spectral density functions of a complex-valued signal $p(t)$ are defined in terms of the conventional spectral density functions [2], as

$$\begin{aligned} S_{pp}(\omega) &= S_{yy}(\omega) + S_{zz}(\omega) + j\left(S_{yz}(\omega) - S_{zy}(\omega)\right) \\ &= S_{yy}(\omega) + S_{zz}(\omega) - 2\cdot\mathrm{Im}\left\{S_{yz}(\omega)\right\} \\ S_{\bar{p}p}(\omega) &= S_{yy}(\omega) - S_{zz}(\omega) + j\left(S_{yz}(\omega) + S_{zy}(\omega)\right) \\ &= S_{yy}(\omega) - S_{zz}(\omega) + j\cdot 2\cdot\mathrm{Re}\left\{S_{yz}(\omega)\right\} \end{aligned} \tag{7}$$

Here, the quantity $S_{pp}(\omega)$ is called the directional power spectral density function (dPSD), whereas $S_{\bar{p}p}(\omega)$ is called the directional cross-spectral density function (dCSD). For the real random signals, the spectral density functions satisfy such symmetric properties as

$$S_{yy}(-\omega) = \bar{S}_{yy}(\omega) = S_{yy}(\omega), \; S_{yz}(-\omega) = \bar{S}_{yz}(\omega) = S_{zy}(\omega) \tag{8}$$

which implies that the conventional PSD, $S_{yy}(\omega)$, is a real, even function of ω, whereas the conventional CSD, $S_{yz}(f)$, is a complex-valued, conjugate even function of ω. Thus, the directional spectra satisfy

$$S_{pp}(-\omega) = S_{\bar{p}\bar{p}}(\omega) \;, \; S_{p\bar{p}}(\omega) = \bar{S}_{\bar{p}p}(\omega) = S_{p\bar{p}}(-\omega) \tag{9}$$

which suggests that the dPSD, $S_{pp}(\omega)$, of a complex signal is a real, but not necessarily even function of ω and the dCSD, $S_{p\bar{p}}(\omega)$, is a conjugate even function of ω. And, the dPSD has the nonnegative property, that is,

$$S_{pp}(\omega) \;\geq\; 0 \tag{10}$$

Now let us consider a complex multiple-harmonic signal representing a periodic planar motion given by,

$$p(t) = \sum_{k=1}^{m}\left\{r_k^b \exp\left[j\left(-\omega_k t\right)\right] + r_k^f \exp\left[j\left(\omega_k t\right)\right]\right\} \tag{11}$$

where m is the number of harmonic components of interest. Now let us consider only the k-th harmonic component, as illustrated in Figure 1. From equation (7), we obtain the corresponding dPSD and dCSD, respectively, as

$$S_{pp}(\omega)=\sum_{k=1}^{m}2\pi\left[\left|r_k{}^f\right|^2\delta(\omega-\omega_k)+\left|r_k{}^b\right|^2\delta(\omega+\omega_k)\right] \tag{12}$$

$$S_{\bar{p}p}(\omega)=\sum_{k=1}^{m}2\pi\left[\left|r_k{}^f\right|\left|r_k{}^b\right|e^{j(\phi^f+\phi^b)}\delta(\omega-\omega_k)+\left|r_k{}^f\right|\left|r_k{}^b\right|e^{j(\phi^f+\phi^b)}\delta(\omega+\omega_k)\right]$$

which consists of two delta functions at $\omega = \omega_k$ and $\omega = -\omega_k$. The dPSD, $S_{pp}(\omega)$, can give not only the separation of forward and backward directional components but also the directivity of each harmonic planar motion. On the other hand, The dCSD, $S_{\bar{p}p}(\omega)$, leads to give the inclination angle ϕ_{inc} through the argument of $S_{\bar{p}p}(\omega)$, i.e.

$$\phi_{inc}(\omega)=\frac{1}{2}\tan^{-1}\left(\frac{\mathrm{Im}\{S_{\bar{p}p}(\omega)\}}{\mathrm{Re}\{S_{\bar{p}p}(\omega)\}}\right)=\frac{1}{2}\left(\phi^f(\omega)+\phi^b(\omega)\right) \tag{13}$$

EXPERIMENTAL SET-UP

Figure 2 shows the laboratory test rotor system [10]. The shaft, which is 10 mm in diameter and 500 mm in length, is supported by two identical deep groove ball bearings. And a rigid disk is located at the mid span of the shaft. A 30 mm long axisymmetric rubber coupling was used as the coupling element, which was found to be very flexible relative to the shaft.

The test rig consisted of two translation stages with the movable range of 0.01 mm to 6.5 mm in the vertical and horizontal directions as shown in Figure 2. The initial shaft alignment was carefully achieved by adjusting the two translation stages so that the fundamental natural frequencies of the rotor system in the y and z directions are equally minimized and the circular whirling orbits are observed in the operating speed range. Using the carefully aligned rotor system with the two translation stages, various angular misalignments with less than 0.02 mm positioning error were imposed at the two ball bearing locations.

RESULTS AND DISCUSSION

Figure 3 shows the whirling orbit measured at the mid-span, along with the 1X(synchronous to the machine running speed) and 2X filtered orbits, as the angular misalignment of $\Delta z_a = 2.0$ mm is applied. The 1X (2X) orbit shows a nearly forward circular (a forward elliptic) whirling motion. Note that the whirling orbit of the test rig with the angular misalignment contains the high level of 2X vibration component, which is known to be a typical characteristics due to misalignment [9]. In particular, the inclination angle made by the major axis of the 2X orbit well coincides with the misalignment direction along the horizontal direction. Figure 4 shows the directional power- and cross-spectra, from which we can easily identify the well-separated backward and forward harmonic components, and the directivity. The magnitudes of directional harmonic components of interest were obtained by calculating the area under the corresponding spectral peak. The SDI indices for the 1X and 2X components were found to be 0.94 and 0.18, respectively. Note that the directional cross spectrum well represents the inclination angle of the 2X harmonic component. Note that the inclination angle of a nearly circular planar motion is very susceptible to the quality of data.

CONCLUSIONS

A vibration signal processing technique is applied to diagnosis of misalignment utilizing the directional spectra of complex-valued signals representing the planar motion. The experimental results confirm that the angular misalignment in a test rig can be effectively identified by using the directional spectra.

REFERENCES

1 Lee, C.W., Vibration Analysis of Rotors, Kluwer Academic Publishers, 1993.

2 Lee, C.W., Joh, Y.D., "A New Horizon in Modal Testing of Rotating Machinery," Keynote Paper, The Fourth Asia-Pacific Vibration Conference, Melbourne, Nov., 1991

3 Lee, C.W., Joh, C.Y., "Use of Directional Spectra for Diagnosis of Asymmetry/ Anisotropy in Rotor Systems," Fourth International Conference on Rotor Dynamics, Chicago, Sep., 1994, pp.97-101.

4 Lee, C.W., Park, J.P., and Han, Y.S., "Use of Directional AR and ML Spectra for Detection of Misfired Engine Cylinder," Fifteenth Biennial ASME Conference on Vibration and Noise, Vol. 3, Part A, DE-Vol. 84-1, 1995, pp.1397-1403.

5 Joh, C.Y., and Lee, C.W., "Use of dFRFs for Diagnosis of Asymmetry/Anisotropy Properties in Rotor-Bearing System," ASME J. of Vibration and Acoustics,, Vol.118, No.1, 1996, pp.64-69.

6 Lee, C.W., Park, J.P., "Inner Race Fault Detection in Rolling Element Bearings by Using Directional Spectra of Vibration Signals, " Sixth International Conference on Vibrations in Rotating Machinery, Oxford, U.K., Sep., 1996, pp.361-370.

7 Lee, C.W., Han, Y.S., " Transient Engine Vibration Analysis by using Directional Wigner Distribution, " SAE Noise and Vibration Conference, Traverse City, May, 1997.

8 Southwick, D.," Using Full Spectrum Plots," Orbit, Vol.14, No.4, Dec., 1993, pp19-21.

9 Goodwin, M.J., Dynamics of Rotor-Bearing Systems, London:Unwin Hyman Ltd.,1989.

10 Lee, Y.S., Lee, C.W., " Effect of Misalignment on Vibration Characteristics of Misaligned Rotor-Ball bearing Systems," Submitted to Journal of Sound and Vibration.

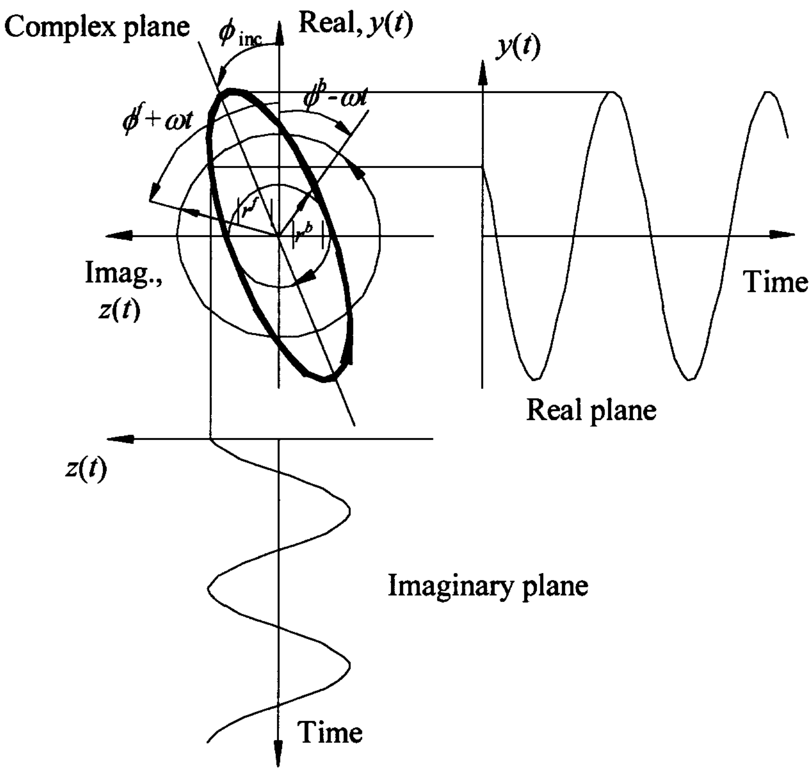

Figure 1 Representation of a complex-valued signal as the sum of two contra-rotating vectors

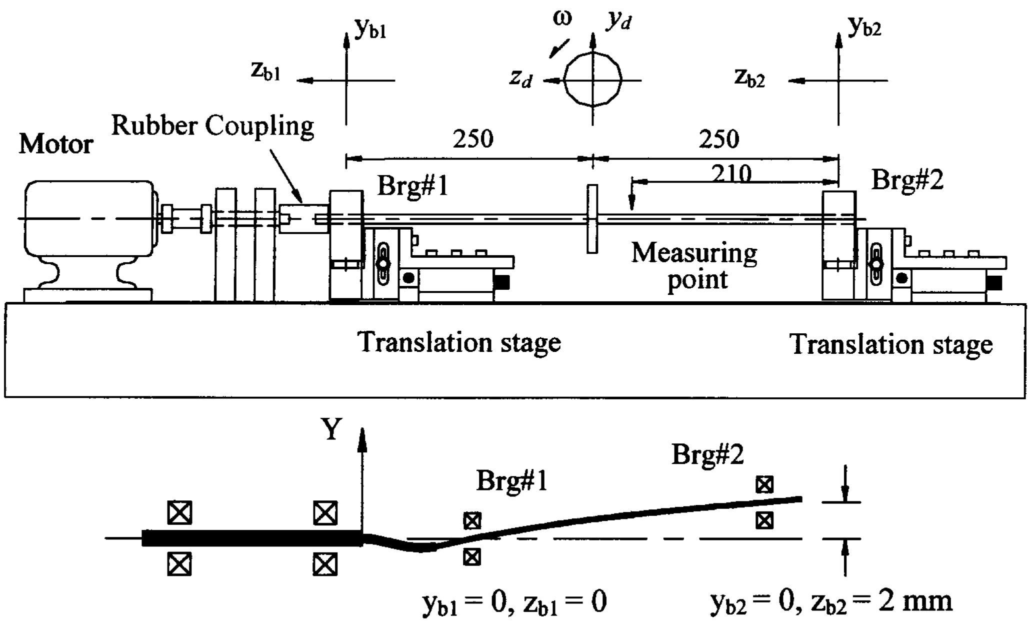

Figure 2 Experimental setup and type of angular misalignment ($\Delta z_a = z_{b2} - z_{b1} = 2.0$ mm)

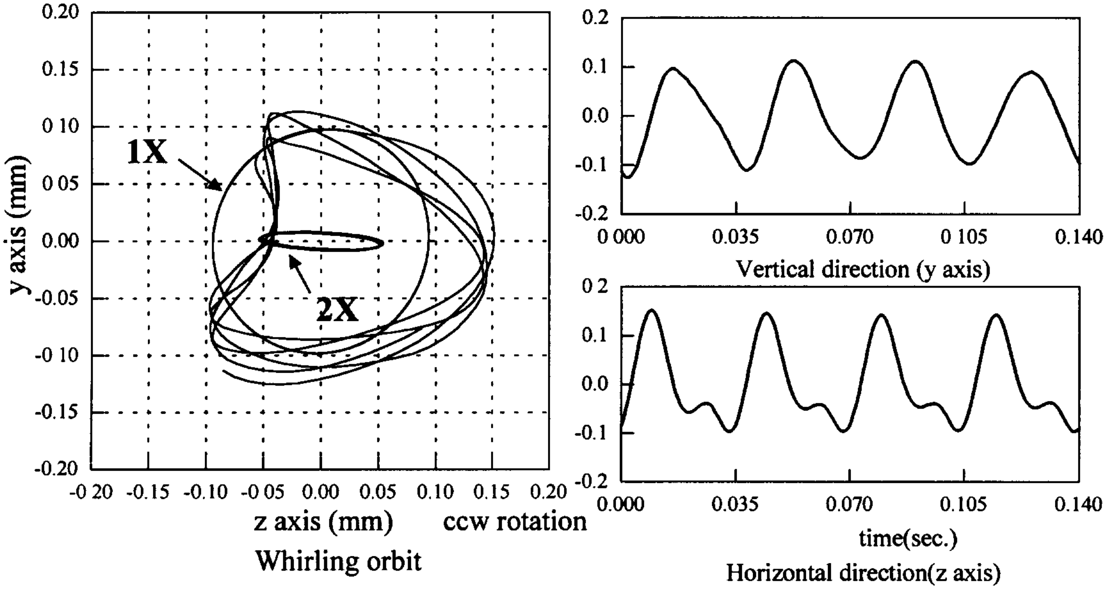

Figure 3 Whirling orbits and time histories at 1700 rpm: angular misalignment $\Delta z_a = 2.0$ mm

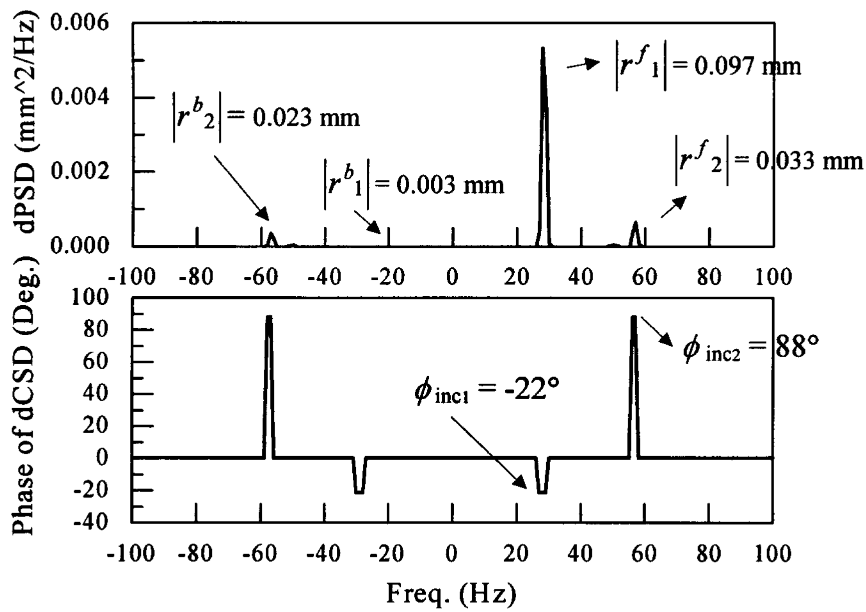

Figure 4 Directional power and cross spectra of complex-valued signal for angular misalignment.